DOI: 10.1002/ejic.200700285

Rarely Decorated Rutile Frameworks Built from Triangular Organic Spacers and Distorted Octahedral Co_3 Building Blocks

Feng Luo,[a] Yun-xia Che,[a] and Ji-min Zheng*[a]

Keywords: Solvothermal syntheses / Rutile / Cobalt / Polymers

Under mild temperatures, the self-assembly of $CoCl_2$ and H_3BTC in a solution of dmso generates a guest-free metal–organic polymer, namely $Co_3(BTC)_2(\mu_1\text{-dmso})_2(\mu_2\text{-dmso})_2$(**1**: dmso = dimethylsulfoxide, H_3BTC = 1,3,5-benzenetricarboxylic acid). In **1**, the Co^{II} ions show the six-coordinate octahedral geometry completed by the BTC^{3-} ions and the dmso oxygen atoms; remarkably, the coordinated dmso ligands not only act as terminal ligands to complete the octahedral geometry of the Co^{II} ions, but also play an important role in bridging Co^{II} ions together to give the Co_3 secondary building units (SBUs). From a topological viewpoint, this novel polymer is classified to be the decorated (3,6)-connected rutile net with the $(4.6^2)_2(4^2.6^{10}.8^3)$ topology, where BTC^{3-} ligands and Co_3 SBUs are viewed to be the 3- and 6-connected nodes, respectively. In addition, the magnetic properties of **1** are explored by using a linear trinuclear cobalt mode, thus leading to $g = 2.41$, $J = -34.92$ cm^{-1}, TIP = 340×10^{-6} cm^3 mol^{-1}, $\theta = -6$ K (a θ parameter was included to take into account intertrinuclear interactions).

Introduction

The design and synthesis of metal-organic frameworks (MOFs) is now of great interest owing to the potential applications and unusual topologies of these new materials.[1] Although this relatively new field of chemistry is aimed at the discovery and synthesis of new materials for practical applications with an emphasis on their functional aspects, it would be difficult to achieve true advancements without an understanding of the structural aspects of these materials at the molecular or atomic levels; however, recent remarkable research results and reviews on framework topologies and other geometrical characteristics of network solids reflect this importance.[2] It seems that for the majority of 3D metal–organic framework topologies, we can find the well-known prototypes in metallic or binary inorganic solids. For example, diamond or diamond-related nets that are composed of tetrahedral nodes are the most common, and they allow the highest interpenetration. A primitive cubic (**pcu**) net/or α-Po net, based on octahedral nodes is also frequently observed and shows the relatively lower two- or threefold interpenetration.[2a,3] Other 3D structures have recently been reported to have the following topologies: boracite, $CdSO_4$, CaB_6, feldspar, NbO, perovskite, Pt_3O_4, PtS, pyrite, quartz, rutile (**rtl**), sodalite, $SrSi_2$, and tungsten bronze.[4] Among the most important and frequently encountered mixed connectivity types, the rutile form of TiO_2 is an important (3,6)-connected net structure. To construct such a net, it appears that assembling triangular building blocks with octahedral building blocks will realize it. In this regard, several compounds with expanded (increased spacing between vertices in a network) **rtl** nets were constructed, most of which are interpenetrating structures constructed with cyano ligands.[5] By contrast, the decorated (replacement of a vertex in a net by a group of vertices) **rtl** nets are less developed. To the best of our knowledge, there are only four interpenetrating decorated and one noninterpenetrating such species.[3b,6] Hence, further investigation into the self-assembly of MOFs characterized by the noninterpenetrating decorated **rtl** nets is needed.

Very recently, most of the significant MOFs were prepared by solvothermal syntheses in CH_3OH, C_2H_5OH, and CH_3CN solutions, but especially in DMF solution.[7] However, the solvothermal synthesis of MOFs in dmso solution is unexplored. Herein, we report such a reaction, and the resulting elegant MOF presents as the second noninterpenetrating decorated **rtl** net.

Results and Discussion

The as-synthesized samples are air-stable and insoluble in water and common organic solvents, such as CH_3OH, C_2H_5OH, CH_3CN, and DMF. Incidentally, dmso decomposes at high temperature and emits a terrible odor; hence, we must be careful to obtain crystal samples from the reaction vessel.

Crystal Structure and Network Topology

Single-crystal X-ray structural analysis revealed that **1** crystallizes in the monoclinic system, space group $P2(1)/c$.

[a] Department of Chemistry, Nankai University, Tianjin, 300071 China
E-mail: jmzheng@nankai.edu.cn

There are two crystallographically independent cobalt ions in this structure. The local coordination geometry for the six-coordinate Co1 center is close to an octahedron coordinated by four BTC^{3-} oxygen atoms and two dmso oxygen atoms. Co2 located at an inverse center is also surrounded by four BTC^{3-} oxygen atoms and two dmso oxygen atoms to give the CoO_6 octahedral geometry. The $Co–O_{dmso}$ bond lengths vary from 2.097 to 2.243 Å, which are comparable to the $Co–O_{carboxylate}$ bond lengths in the range of 2.034–2.228 Å, and both of them are comparable with those observed in other Co–BTC compounds;[13] thus, the distortion parameter of the CoO_6 octahedra is 8.8×10^{-4} for Co1 and 2.2×10^{-3} for Co2.[8] As for each BTC^{3-} ligand, it shows a pentadentate-coordinated mode with one carboxyl group chelated to the Co1 ion and two carboxyl groups bridging Co1 with Co2.

The Co1, Co2, and symmetry-related Co1′ ions are combined together by the *syn-syn* carboxyl groups of the BTC^{3-} ligands and μ_2-dmso bridges thus leading to the linear Co_3 SBU of corner-sharing octahedra (Figure 1). The intratrinuclear Co1–Co2 distance is 3.562 Å, and the $Co1–O_{dmso}–Co2$ angle is 109.04°. Furthermore, each SBU connects six BTC^{3-} ligands in six directions (Figure 2), whereas each BTC^{3-} ligand ligates three SBUs (Figure 3); consequentially, such a connectivity pattern is repeated infinitely to construct the infinite (3, 6)-connected net (Figure 4). For perspicuous representation, the Co_3 SBUs are represented by distorted octahedral nodes, as each carboxyl group is more-or-less offset from the phenyl plane and not all the vertices of each octahedral Co_3 SBU are symmetrically equivalent, whereas the BTC^{3-} ligands are described as triangular units.

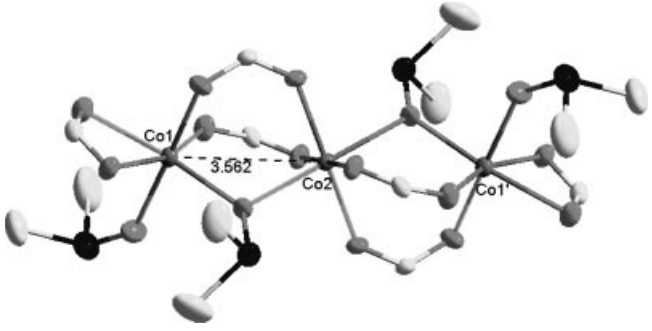

Figure 1. Schematic description of the Co_3 SBU and its coordinated environment: C is light grey, S is black, and O is dark grey. The atoms are drawn at the 50% probability level.

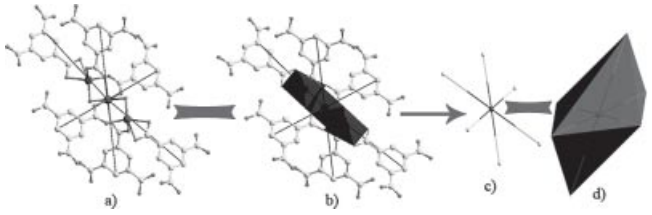

Figure 2. a) Ball-and-stick mode of the six-connected Co_3 SBU; b) polyhedral illustration of the Co_3 core; c) the simplified node-to-node fashion of the six-connected SBU; d) polyhedral illustration of the distorted octahedral SBU.

Hence, the framework should be viewed as a noninterpenetrating decorated **rtl** net with the $(4.6^2)_2(4^2.6^{10}.8^3)$ topology, where six-connected Co_3 SBUs and three-connected BTC^{3-} units correspond to the Ti atoms and the O atoms in the **rtl** net structure, respectively.

Figure 3. a) Ball-and-stick mode of the three-connected BTC^{3-} unit; b) polyhedral illustration of the Co_3 core; c) the simplified node-to-node fashion of the triangle BTC^{3-} node.

Figure 4. View of the noninterpenetrating decorated rutile net with the $(4.6^2)_2(4^2.6^{10}.8^3)$ topology and constructed from distorted octahedral Co_3 SBUs and triangle BTC^{3-} units.

Carefully checking the reported decorated **rtl** nets, we find that most of them are built from octahedral M_2 (M = metal ion) SBUs and triangular organic units. Obviously, the present one contains the biggest octahedral SBUs (Co_3).

Magnetic Properties

The $\chi_M T$ product of crystal samples of **1** was measured in the temperature range 2–300 K with applied magnetic fields of 500 Oe (Figure 5). At room temp., the $\chi_M T$ value of 6.37 $cm^3 K mol^{-1}$ is slightly higher than that of three high-spin Co^{II} ion (5.63 $cm^3 mol^{-1} K$, $S = 3/2$, $g = 2.0$) as a magnetically noninteracting center owing to orbital contribution from the octahedral high-spin Co^{II} ions. Upon cooling from room temp., the $\chi_M T$ product linearly decreases to 2.30 $cm^3 K mol^{-1}$ at 10 K, which is due to the spin-orbit coupling effects of the high-spin octahedral Co^{II} ions with an orbital degenerate $^4T_1$ ground term and the antiferromagnetic exchange coupling between Co^{II} ions. The $\chi_M T$ values then sharply decrease to 1.19 $cm^3 K mol^{-1}$ at 2 K as a result of the ZFS (zero field splitting) and/or other fac-

tors, such as intertrinuclear interactions. In the $1/\chi_M$ versus T plot, above 75 K, the plot is exactly a straight line well-fitted by the Curie–Weiss law [$\chi_M = C/(T - \theta)$], with C = 8.3 $cm^3 mol^{-1} K$ and θ = –83.0 K. This is consistent with three S = 3/2 Co^{II} ions with moderate antiferromagnetic coupling to yield an average g value of 2.4. This large Weiss constant indicates a dominated antiferromagnetic coupling between the Co^{II} ions.

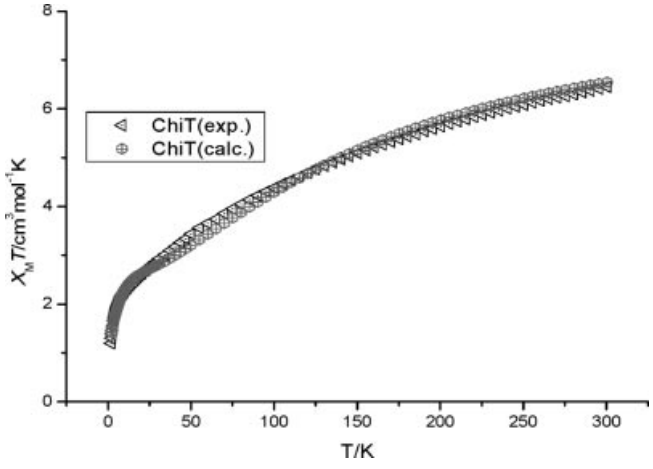

Figure 5. The plot of $\chi_M T$ vs. T: open triangle is the experimental curve and the crossed circle is the simulated curve.

As mentioned above, in this linear Co_3 unit, Co1 and Co1′ are symmetrical, and the closest distance of Co1–Co1′ is 7.124 Å; hence, we chose a "one J" mode to analyze the experimental magnetic data.[9] A least-squares fit to the data leads to g = 2.41, J = –34.92 cm^{-1}, TIP = 340×10^{-6} $cm^3 mol^{-1}$, ρ = 0.09 $cm^3 mol^{-1} K$, and θ = –6 K: J is the magnetic coupling parameter between Co1–Co2 and Co1′–Co2, g is the Zeeman factor, TIP is the temperature-independent paramagnetism, ρ is the paramagnetic impurity, and θ is the intertrinuclear interactions. It is not surprising to find important TIP contributions and such a strong Zeeman factor. Indeed, the combined influences of the local distortion of the coordination sphere around the Co^{II} ion and the spin-orbit coupling are known to produce this set of local parameters.[10]

Relative to the pyridazine-bridging Co3 compounds,[11] the preset compound bridged by μ_2-O atoms displays the obviously bigger antiferromagnetic interactions, but comparable with the cobalt(II)–hydroxy compounds.[12]

TGA Research of 1

The TG research (30–800 °C) of **1** shows that at 30–300 °C, there is no weight loss, which is consist with the structure of **1**, and polymer **1** then starts to perform the process of chemical decomposition (Figure 6). The remains may be Co_2O_3 (calcd. 28%; found 30%).

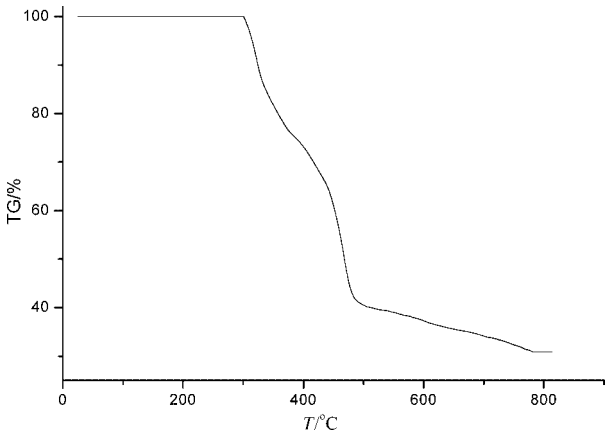

Figure 6. The TG plot of **1** (to our surprise, we found that the TG plot is straight until 300 °C; maybe, the former treatment such as heating to avoid the absorbed water molecules and N_2 protection are the main reason.

Conclusions

Through this original research, we initiated the solvothermal synthesis of MOFs in dmso solution. The resulting MOF, defined as a noninterpenetrating decorated rutile net with the $(4.6^2)_2(4^2.6^{10}.8^3)$ topology, is built from distorted octahedral Co_3 SBUs and triangular BTC^{3-} units. To the best of knowledge, this distorted octahedral Co_3 SBU is the biggest relative to those (M_2 SBU) observed in other similar instances. In addition, it should be highlighted that the dmso molecules in polymer **1** display two different ligand coordination modes: terminal and μ_2-bridging; however, this phenomenon has never been observed in the literature. Thus, this study will largely enrich the field of MOFs and further understand the coordinated behavior of H_3BTC ligands, especially the dmso molecules.

Experimental Section

Materials and Instrumentation: All reagents were bought from commercial sources and used without further purification. Elemental analysis was carried out with an Elementar Vario ELIII microanalyzer. Magnetic measurements were carried out with a Quantum

Table 1. Crystal and structure refinement data for **1**.

Complex	**1**
Formula	$C_{26}H_{30}Co_3O_{16}S_4$
Fw	903.53
Crystal system	monoclinic
Space group	$P2_1/c$
a / Å	10.107(2)
b / Å	10.258(2)
c / Å	16.276(3)
β / °	95.38(3)
V / $Å^3$	1680.0(6)
Z	2
$D_{calcd.}$ / $g cm^{-3}$	1.786
S	1.032
R_1[a]	0.0625
ωR_2[b]	0.1406

[a] $R_1 = \Sigma|F_o - F_c|/\Sigma|F_o|$. [b] $\omega R_2 = \Sigma[\omega(F_o^2 - F_c^2)^2]/\Sigma[\omega(F_o^2)^2]^{1/2}$.

Table 2. Selected bond lengths [Å] and angles [°] for **1**.[a]

Co1–O1	2.034(4)	O4#2-Co1–O6#3	86.34(16)
Co1–O4#2	2.054(4)	O7–Co1–O6#3	90.48(17)
Co1–O7	2.096(4)	O1–Co1–O8#4	97.16(15)
Co1–O6#3	2.113(4)	O4#2-Co1–O8#4	90.22(16)
Co1–O8#4	2.131(4)	O7–Co1–O8#4	89.97(15)
Co1–O5#3	2.228(4)	O6#3-Co1–O8#4	102.19(15)
Co2–O3#5	2.042(3)	O1–Co1–O5#3	99.97(15)
Co2–O3#2	2.042(3)	O4#2-Co1–O5#3	86.38(16)
Co2–O8#4	2.243(4)	O7–Co1–O5#3	92.49(16)
Co2–O8	2.243(4)	O6#3-Co1–O5#3	60.64(14)
O3–Co2#6	2.042(3)	O8#4-Co1–O5#3	162.66(14)
O4–Co1#6	2.054(4)	O2#4-Co2–O2	180.0(3)
O5–Co1#1	2.228(4)	O2#4-Co2–O3#5	89.76(16)
O1–Co1–O(4)#2	92.37(16)	O2–Co2–O3#5	90.24(16)
O1–Co1–O7	90.79(18)	O2#4-Co2–O8#4	88.48(15)
O4#2-Co1–O7	176.78(18)	O2–Co2–O8#4	91.52(15)
O1–Co1–O6#3	160.61(15)	O3#5-Co2–O8#4	84.18(14)
		O3#2-Co2–O8#4	95.82(14)

[a] Symmetry transformations used to generate equivalent atoms: #1: $x - 1$, y, z; #2: $-x + 2$, $y - 1/2$, $-z + 1/2$; #3: $x + 1$, y, z; #4: $-x + 2$, $-y$, $-z$; #5: x, $-y + 1/2$, $z - 1/2$; #6: $-x + 2$, $y + 1/2$, $-z + 1/2$.

Design (SQUID) magnetometer MPMS-XL-5. Thermal gravimetric analysis was completed with a NETZSCH TG 209 instrument.

Preparation of 1: A mixture of $CoCl_2 \cdot 6H_2O/H_3BTC$ (1:0.8) in a solution of dmso (10 mL) was placed in a Teflon reactor (23 mL) and heated at 160 °C for 3 d. The mixture was then cooled to room temp. at 5 °C h^{-1}. Purple crystals were obtained in 75% yield based on Co. $C_{26}H_{30}Co_3O_{16}S_4$ (903.53): calcd. C 34.56, H 3.35; found C 34.52, H 3.26.

X-ray Crystallographic Studies: Intensity data were collected with a rigaku r-axis rapid IP area detector with Mo-K_α monochromated radiation (λ = 0.71073 Å) at room temp. Empirical absorption correction was applied. The structures of these polymers were solved by direct method and refined by full-matrix least-squares on F^2 by using the SHELXL-97 software. All of the non-hydrogen atoms were refined anisotropically. The organic hydrogen atoms were generated geometrically and refined with isotropic temperature factors. Crystal data and structure refinement for these polymers are summarized in Table 1. Selected bond lengths and angels are listed in Table 2. CCDC-638904 contains the supplementary crystallographic data for this paper. These data can be obtained free of charge from The Cambridge Crystallographic Data Centre via www.ccdc.cam.ac.uk/data_request/cif.

Acknowledgments

This work was supported by the National Natural Science Foundation of China under Project 50572040.

[1] a) P. J. Hagrman, D. Hagrman, J. Zubieta, *Angew. Chem. Int. Ed.* **1999**, *38*, 2638; b) A. J. Blake, N. R. Champness, P. Hubberstey, W. S. Li, M. A. Withersby, M. Schröder, *Coord. Chem. Rev.* **1999**, *183*, 117; c) B. Moulton, M. J. Zaworotko, *Chem. Rev.* **2001**, *101*, 1629; d) O. R. Evans, W. Lin, *Acc. Chem. Res.* **2002**, *35*, 511; e) O. M. Yaghi, M. O'Keeffe, N. W. Ockwig, H. K. Chae, M. Eddaoudi, J. Kim, *Nature* **2003**, *423*, 705; f) C. N. R. Rao, S. Natarajan, R. Vaidhyanathan, *Angew. Chem. Int. Ed.* **2004**, *43*, 1466; g) S. Kitagawa, R. Kitaura, S. I. Noro, *Angew. Chem. Int. Ed.* **2004**, *43*, 2334.

[2] a) S. R. Batten, R. Robson, *Angew. Chem. Int. Ed.* **1998**, *37*, 1460; b) M. O'Keeffe, M. Eddaoudi, H. Li, T. Reineke, O. M. Yaghi, *J. Solid State Chem.* **2000**, *152*, 3; c) R. Robson, *J. Chem. Soc. Dalton Trans.* **2000**, 3735; d) M. Eddaoudi, D. B. Moler, H. Li, B. Chen, T. M. Reineke, M. O'Keeffe, O. M. Yaghi, *Acc. Chem. Res.* **2001**, *34*, 319; e) B. Moulton, M. Zaworotko, *Chem. Rev.* **2001**, *101*, 1629; f) O. R. Evans, W. Lin, *Acc. Chem. Res.* **2002**, *35*, 511; g) O. M. Yaghi, M. O'Keeffe, N. W. Ockwig, H. K. Chae, M. Eddaoudi, J. Kim, *Nature* **2003**, *423*, 705; h) S. L. James, *Chem. Soc. Rev.* **2003**, *32*, 276.

[3] a) D. S. Reddy, T. Dewa, K. Endo, Y. Aoyama, *Angew. Chem. Int. Ed.* **2000**, *39*, 4266; b) V. A. Blatov, L. Carlucci, G. Cianib, D. M. Proserpio, *CrystEngComm* **2004**, *6*, 377; c) F. Luo, S. R. Batten, Y. X. Che, J. M. Zheng, *Chem. Eur. J.* **2007**, *13*, 4948; d) F. Luo, Y. X. Che, J. M. Zheng, *Cryst. Growth Des.* **2006**, *6*, 2432.

[4] a) M. Eddaoudi, J. Kim, D. Vodak, A. Sudik, J. Wachter, M. O'Keeffe, O. M. Yaghi, *Proc. Natl. Acad. Sci. USA* **2002**, *99*, 4900; b) J. Kim, B. Chen, T. M. Reineke, H. Li, M. Eddaoudi, D. B. Moler, M. O'Keeffe, O. M. Yaghi, *J. Am. Chem. Soc.* **2001**, *123*, 8239; c) M. Eddaoudi, J. Kim, M. O'Keeffe, O. M. Yaghi, *J. Am. Chem. Soc.* **2002**, *124*, 376; d) B. Chen, M. Eddaoudi, S. T. Hyde, M. O'Keeffe, O. M. Yaghi, *Science* **2001**, *291*, 1021; e) B. Chen, M. Eddaoudi, T. M. Reineke, J. W. Kampf, M. O'Keeffe, O. M. Yaghi, *J. Am. Chem. Soc.* **2000**, *122*, 11559.

[5] a) S. R. Batten, B. F. Hoskins, R. Robson, *J. Chem. Soc. Chem. Commun.* **1991**, 445; b) S. R. Batten, B. F. Hoskins, B. Moubaraki, K. S. Murray, R. Robson, *J. Chem. Soc. Dalton Trans.* **1999**, 2977; c) P. Jensen, D. J. Price, S. R. Bateen, B. Moubaraki, K. S. Murray, *Chem. Eur. J.* **2000**, *6*, 3186; d) L. Carlucci, G. Ciani, F. Porta, D. M. Proserpio, L. Santagostini, *Angew. Chem. Int. Ed.* **2002**, *41*, 1907; e) F. C. Liu, Y. F. Zeng, J. Jiao, X. H. Bu, J. Ribas, S. R. Batten, *Inorg. Chem.* **2006**, *45*, 2776; f) D. B. Cordes, L. R. Hanton, *Inorg. Chem.* **2007**, *46*, 1634; g) S. Hu, A. J. Zhou, Y. H. Zhang, S. Ding, M. L. Tong, *Cryst. Growth Des.* **2006**, *6*, 2543; h) J. Luo, X. G. Zhou, X. F. Hou, H. X. Wu, L. H. Weng, Y. R. Li, *Chin. J. Chem.* **2005**, *23*, 310; i) C. Qin, X. L. Wang, E. B. Wang, Z. M. Su, *Inorg. Chem.* **2005**, *44*, 7122; j) J. A. Schlueter, J. L. Manson, U. Geiser, *Inorg. Chem.* **2005**, *44*, 3194.

[6] a) I. Ino, P. L. Wu, M. Munakata, Y. Maekawa, Y. Suenaga, I. Kuroda-Sowa, Y. Kitamori, *Inorg. Chem.* **2000**, *39*, 2146; b) M. Schwarten, J. Chomic, J. Cernak, D. Babel, *Z. Anorg. Allg. Chem.* **1996**, *622*, 1478; c) L. H. Xie, S. X. Liu, B. Gao, C. D. Zhang, C. Y. Sun, D. H. Li, Z. M. Su, *Chem. Commun.* **2005**, 2402; d) C. Qin, X. L. Wang, L. Carlucci, M. L. Tong, E. B. Wang, C. W. Hu, L. Xu, *Chem. Commun.* **2004**, 1876.

[7] a) H. Chun, D. Kim, D. N. Dybtsev, K. Kim, *Angew. Chem. Int. Ed.* **2004**, *43*, 971; b) X. S. Wang, S. Ma, D. Sun, S. Parkin,

H. C. Zhou, *J. Am. Chem. Soc.* **2006**, *128*, 16474; c) B. Chen, S. Ma, F. Zapata, E. B. Lobkovsky, J. Yang, *Inorg. Chem.* **2006**, *45*, 5718.
[8] N. E. Khayati1, R. C. El Moursli, J. RodrÍguez-Carvajal, G. André, N. Blanchard, F. Bourée, G. Collin, T. Roisnel, *Eur. Phys. J. B* **2001**, *22*, 429.
[9] MAGMUN was developed by Dr. Zhiqiang Xu and OW01.exe by Dr. O. Waldmann.
[10] a) O. Kahn, *Molecular Magnetism*, VCH, New York, **1993**; b) N. Benbellat, K. S. Gavrilenko, Y. Le Gal, O. Cador, S. Golhen, A. Gouasmia, J. M. Fabre, L. Ouahab, *Inorg. Chem.* **2006**, *45*, 10440; c) A. Rodriguez-Dieguez, R. Kivekas, R. Sillanpaa, J. Cano, F. Lloret, V. McKee, H. Stoeckli-Evans, E. Colacio, *Inorg. Chem.* **2006**, *45*, 10537.
[11] a) S. Brooker, D. J. de Geest, R. J. Kelly, P. G. Plieger, B. Moubaraki, K. S. Murray, G. B. Jameson, *J. Chem. Soc. Dalton Trans.* **2002**, 2080; b) U. Beckmann, S. Brooker, *Coord. Chem. Rev.* **2003**, *245*, 17.
[12] Y. Z. Zheng, M. L. Tong, W. X. Zhang, X. M. Chen, *Chem. Commun.* **2006**, 165.
[13] Y. Y. Liu, J. F. Ma, J. Yang, Z. M. Su, *Inorg. Chem.* **2007**, *46*, 3027.

Received: March 13, 2007
Published Online: June 29, 2007

